Sensors and Actuators B: Chemical, Volume 228, 2 June 2016, pp573-580
DOI: 10.1016/j.snb.2016.01.058

A long period grating optical fiber sensor with nano-assembled porphyrin layers for detecting ammonia gas

Tao Wang,[1] Sergiy Korposh,[2] Stephen W. James,[3] Ralph P. Tatam,[3]
and Seung-Woo Lee[1*]

[1] *Graduate School of Environmental Engineering, The University of Kitakyushu, 1-1 Hibikino, Kitakyushu 808-0135, Japan*
[2] *Department of Electrical and Electronic Engineering, University of Nottingham, Nottingham, NG7 2RD, UK*
[3] *Department of Engineering Photonics, School of Engineering, Cranfield University, Cranfield, Bedford MK43 0AL, UK*

* Corresponding author. Tel.: +81-93-695-3293; fax: +81-93-695-3384; e-mail: leesw@kitakyu-u.ac.jp

Abstract

In this study, the ability of a long period grating (LPG) optical fiber sensor coated with a multilayer film of poly(diallyldimethyammonium chloride) (PDDA) and tetrakis(4-sulfophenyl)porphine (TSPP) to detect ammonia gas was demonstrated. The nano-assembled thin film was prepared using a layer-by-layer deposition technique. This combination of an LPG and TSPP could allow highly sensitive optical sensors that specifically bind ammonia to be fabricated. An LPG with a period of 100 µm and a PDDA/TSPP coating produced by depositing 15 layers afforded a limit of detection of 0.67 ppm for ammonia gas. TSPP molecules in the film acted as ammonia receptors because the TSPP morphologically changed from *J*- or *H*-aggregates to free base monomers when it was deprotonated by being exposed to ammonia. Interestingly, HCl vapor could be used to increase the relative amount of *J*-aggregation in the TSPP and to restore the sensor response. The reversibility of the morphological change in the TSPP allowed reversible changes to occur in the properties of the coating, including the refractive index, film thickness and density, and electrostatic interactions; these influenced the transmission spectrum of the LPG.

Keywords: Long period grating (LPG), optical fiber, porphyrin, self-assembly, ammonia, refractive index

1. Introduction

Ammonia is an important chemical that is widely used in the chemical industry. Reliable detection of ammonia over a wide concentration range is necessary. Humans can smell ammonia at a concentration of about 55 ppm [1], particularly when exposed to it for the first time. However, repeated exposure causes inurement effects, and people regularly exposed to ammonia become less sensitive to its smell. The US National Institute for Occupational Safety and Health have recommended exposure limits of 35 ppm for general occupational exposure and 50 ppm for exposure in the industrial sector [2], and these limits are close to or below the concentrations at which humans can potentially smell ammonia.

The use of ammonia as a potential disease biomarker has recently attracted the attention of researchers. Ammonia in the human body is mainly produced through the metabolism of proteins, and the ammonia produced is converted into urea and excreted in the urine [3]. However, ammonia is normally present at low concentrations in the blood, feces, exhaled breath, and skin secretions [4]. The presence of ammonia at atypical concentrations in these media has been suggested to indicate disease, particularly kidney or liver disorders. Numerous investigations have recently been reported wherein the potential has been assessed for using ammonia in human breath as a biomarker for physical disorders such as renal insufficiency [5], hepatic dysfunction [6], *Helicobacter pylori* infection [7], and halitosis [8].

Conventional methods of detecting ammonia usually use gas chromatography-mass spectrometry (GC-MS) [9] because of the selectivity and sensitivity of GC-MS. However, using GC-MS is expensive and time-consuming, and the operator must be well trained. Thus, devices capable of detecting ammonia concentrations of 1–50 ppm in ambient air are often required. Transducers for sensing ammonia that are frequently used include resistive devices, acoustic wave devices, and field-effect transducers [10].

A long period grating (LPG) is a periodic modulation of the refractive index (RI) of the core of an optical fiber that results in the coupling of light between the core and cladding modes. Combining an LPG with nanomaterials could allow highly sensitive sensors that could specifically bind target chemical species to be fabricated [11-13]. We have recently demonstrated that optical fiber LPG sensors modified with different functional coatings can be used to detect ammonia [11, 12], aromatic carboxylic acids [13], and the RI of a sample [14, 15]. The sensitivity of an LPG to the RI arises from the dependence of the phase matching condition on the effective RI of the cladding modes, which is governed by equation 1 [16],

$$\lambda_{(x)} = (n_{core} - n_{clad(x)})\Lambda , \qquad (1)$$

where $\lambda_{(x)}$ is the wavelength at which coupling to the linear polarized (LP_{0x}) mode occurs, n_{core} is the effective RI of the mode propagated in the core, $n_{\mathrm{clad(x)}}$ is the effective RI of the LP_{0x} cladding mode, and Λ is the period of the grating. The phase matching will reach a maximum and exhibit a turning point, at which the sensitivity of the resonance bands in the transmission spectrum of the LPG to perturbations caused by, for example, changes in the RI of a coating deposited onto the fiber reaches a maximum [17]. The phase matching turning point can be determined by selecting an appropriate grating period.

In this study, we examined the performance of an LPG-based ammonia gas sensor modified with a nano-assembled thin film consisting of alternate layers of poly(diallyldimethylammonium chloride) (PDDA) and tetrakis(4-sulfophenyl)porphine

(TSPP). We have previously demonstrated that an evanescent wave spectroscopy-based fiber-optic ammonia gas sensor modified with a TSPP nano-assembled film induced optical changes in the transmission spectrum of the optical fiber when the sensor was exposed to ammonia [18]. The TSPP structures in such a film contain two distinct types of aggregates, called *J*- and *H*-aggregates, together with monomers. The relative abundances of those structures change as the degree to which the TSPP is protonated or deprotonated changes [19-22].

This behavior of the TSPP would lead to changes occurring in the RI of the coating, causing the phase matching conditions, and therefore the transmission spectrum, of an optical fibre LPG modified with a nano-assembled TSPP film to change. Previously, we have exploited this to demonstrate the detection of ammonium in water by creating a sensor consisting of a mesoporous SiO_2 thin film that was deposited onto an LPG[ref A into which the functional material, the TPSS, was infused. Here we use an LPG coated with TSPP using the LbL approach to detect ammonia gas. We report, , for the first time to the best of our knowledge, the measurement in real time of changes in the RI of TSPP LbL thin films at the exposure to the ammonia gas.

2. Experimental section

2.1. Materials

TSPP (*M*w 934.99) and PDDA (*M*w 200,000–350,000, 20 wt% in H_2O) that were used were purchased from Tokyo Kasei (Tokyo, Japan) and Sigma-Aldrich (St Louis, MO, USA), respectively. The TSPP and PDDA chemical structures are shown in Figure 1. Ammonia (ca. 30 wt% in H_2O), for use as an analyte gas, was purchased from Wako Pure Chemical Industries (Osaka, Japan). All of these chemicals were of analytical grade, and they were used without further purification. Deionized pure water (18.3 MΩ·cm) was produced using a Direct-QTM instrument (EMD Millipore, Billerica, MA, USA), which performed reverse osmosis, then ion exchange and filtration.

2.2. LPG surface modification

An LPG of length 30 mm and with a period of 100 μm was fabricated in a boron–germanium co-doped single-mode optical fiber (PS750; Fibercore, Southampton, UK) with a cut-off wavelength of 670 nm, in a point-by-point fashion, side-illuminating the optical fiber using a frequency-quadrupled Nd:YAG laser operated at 266 nm. The period was selected such that the phase matching condition was satisfied at the phase matching turning point. Aqueous solutions containing different sucrose concentrations were used to calibrate the RI-sensitivity of the LPG, as previously described [13, 14].

The region of the optical fiber containing the LPG was rinsed with deionized water and immersed in 1 wt% KOH in a 3:2 v/v mixture of ethanol and water for 20 min, to induce a negatively charged surface before the PDDA/TSPP coating was deposited. The section containing the LPG was then coated with a multilayer PDDA and TSPP film using the layer-by-layer method. A film was prepared by alternately depositing PDDA (0.5 wt% in water, pH=7.8) and TSPP (1 mM in water, pH=4.6) for one cycle, thereby producing a PDDA/TSPP bilayer. To deposit a layer, the coating solution (350 μl) was introduced into a Teflon deposition cell containing a recess (0.5 cm wide, 6.0 cm long, and d 0.3 cm deep). The deposition cell was washed with water and dried by flushing it with nitrogen after each layer had been deposited, as shown in Figure 1. The transmission spectrum (TS) of the LPG was measured after each deposition step had been performed.

A film was also deposited on a quartz plate using a procedure that was essentially identical to that used to deposit a film onto an LPG. The composition of the film was confirmed using UV–vis spectroscopy (using a V-570 UV–vis spectrophotometer; JASCO, Japan). Prior to deposition of the film, a quartz plate was cleaned with concentrated sulfuric acid (96%), rinsed several times with deionized water, treated with 1 wt% KOH in a 3:2 v/v mixture of ethanol and water for a few minutes, rinsed with deionized water, and dried by flushing it with nitrogen gas.

2.3. Gas measurements

The TS of the optical fiber was acquired by passing the output of a tungsten–halogen lamp (HL-2000; Ocean Optics, Dunedin, FL, USA) into the fiber and analyzing the light that was transmitted using a fiber-coupled CCD spectrometer (HR-2000; Ocean Optics). The response of the LPG to ammonia was measured by exposing the LPG to ammonia vapor at different concentrations, generated by placing aqueous solutions of ammonia at different concentrations close to the modified LPG sensor. The relationship between the ammonia vapor concentration and the ammonia concentration in solution is shown in Figure S1. The ammonia concentration was measured using an ammonia detection gas tube (GasTec, Japan). A specified volume of a solution of ammonia at a selected concentration was placed in a 50 cm^3 measurement chamber containing the modified LPG. The sensor response was recorded at a frequency of 1 Hz. The TS was acquired when each analyte solution was present in the chamber and after the solution was removed. The sensor response was restored after a series of ammonia gas measurements had been made by treating the optical fiber with the vapor emitted from a 0.1 M HCl aqueous solution, then the fiber was flushed using nitrogen.

3. Results and discussion

3.1. Deposition of the PDDA/TSPP film

In order to study the effect of the film deposition on the TS of the LPG optical fibre sensor TS was measured after each deposition cycle. The TS of the LPG changed dramatically during the PDDA/TSPP film deposition process. The resonance band at around 745 nm had split into two bands, 711 and 795 nm, by the time the fifteenth deposition step had been completed, as shown in Figures 2a and 2b for the outermost PDDA and TSPP layers, respectively. This band separation was observed after four deposition cycles (of both components, see Figure 2S), and the shifts in the wavelengths of both resonance bands changed linearly as the number of deposition cycles increased, indicating that the film was uniformly deposited (Figure 3a). The mean wavelength shifts for each layer that was deposited were estimated to be −3.27±2.30 nm and 3.90±3.26 nm for the first and second resonance bands, respectively, for PDDA and −2.78±3.26 nm and 4.45±1.99 nm for the first and second resonance bands, respectively, for TSPP (Figure 3b).

It is clear from comparing Figures 3c and 3d that the TS changed more significantly when the outermost layer was TSPP than when the outermost layer was PDDA. Both resonance bands were almost symmetrical when the outermost layer was PDDA but asymmetric when the outermost layer was TSPP. In a previous study, however, we found almost symmetrical wavelength and transmission changes in both resonance bands in the TS of a film deposited using poly(acrylic acid) as a polyanion [11, 12]. Change in the transmission of the first resonance band was independent of the outermost layer material until seven deposition cycles had been completed. Afterwards, it dramatically increased when the outermost layer was TSPP (Figure 3c). In contrast, the transmission of the second resonance band reached a plateau after nine deposition cycles had been completed, especially when the outermost layer was PDDA (Figure 3d). The transmission of the first band in the TS was ca. 63% before the bands separated and reached 77% after 15 TSPP deposition cycles had been performed, so the transmission increased by 14% in total.

Most plausibly these changes in the TS of the LPG are related to the TSPP aggregation structures in the film and their corresponding optical properties. In order to examine this in more detail, the UV–vis absorption spectra of the alternate PDDA and TSPP layers deposited on a quartz plate were used to characterize the TSPP assemblies in the film. The evolution of the UV–vis absorption spectra during the deposition of a PDDA/TSPP thin film over five deposition cycles is shown in Figure 4. The absorption spectra for films with an outermost layer of TSPP were characterized by a double peak in the Soret band at 429 and 485 nm and by a pronounced Q band peak at 700 nm (Figure 4b). However, when the film had an outermost layer of PDDA there was a single peak in the Soret band at 410 nm (Figure 4a). These spectral characteristics suggest that the TSPP molecules in the film were preferentially present in the *J*-aggregate state when the TSPP had just been deposited. The absorbance by the two Soret bands and the Q band increased linearly as the number of deposition cycles increased (inset in Figure 4b). The formation of the *J*-aggregates of TSPP is likely to have increased the RI of the film, influencing the phase matching condition, and therefore, the transmission spectrum of the LPG. An increase in the absorbance of the Q band at around 700 nm was found to lead to an asymmetrical change in the first resonance band in the TS, because the complex part of the refractive index will be strongly influenced by such a change.

3.2. Ammonia detection

3.2.1 J-aggregation state enhancement

In order to increase the population of *J*-aggregates of TSPP in the film before it was exposed to ammonia, the prepared PDDA/TSPP film was exposed to HCl vapor (produced by aqueous 0.1 M HCl). As can be seen from Figure 5, the absorbance of the Soret band at 485 nm and of the Q band at 700 nm were enhanced significantly when the film was treated with HCl, suggesting that exposure to HCl gas increased the relative population of *J*-aggregates of TSPP in the film. It should be noted that pure water vapor has a similar effect to that of HCl on the absorption spectra of the TSPP (i.e. resulting in an increase in the relative population of *J*-aggregates of TSPP in the film and hence in the absorption at 485 nm and 700 nm), but the amplitude will be much smaller (data not shown). After exposure to the HCl, however, further exposure to pure water vapor did not lead to a measurable modification of the absorption spectra.

In the case of the LPG sensor, the HCl pretreatment led to more asymmetrical changes occurring in the TS and the resonance bands at 710 and 785 nm were shifted to 709 and 800 nm, respectively. The transmission of the first resonance band increased significantly, from 67% to 87%. The wavelength of the second resonance band was shifted by a relatively large amount, ca. 15 nm (from 785 to 800 nm).

3.2.2 Response to ammonia gas

When the sensor was exposed to ammonia gas at different concentrations the second resonance band wavelength shifted linearly relative to the ammonia concentration at concentrations of less than 50 ppm (inset in Figure S4a). As can be seen in Figure 6, the wavelength shift in the second resonance band in the HCl-vapor-treated LPG sensor was more sensitive to the effects of exposure to ammonia than were the other TS features. The sensor response became saturated at concentrations higher than 50 ppm. The sensitivity of the sensor to ammonia within the linear range was estimated to be 0.4 %/ppm using the first resonance band and 0.7 nm/ppm using the second resonance band. The limits of detection for the first and second resonance bands were found to be 2.2 ppm ($3\sigma = 0.25\%$) and 3.3 ppm ($3\sigma = 0.47$ nm), respectively.

3.3.3 Refractive index determination

In order to calibrate the LPG sensor to the RI change, the uncoated LPG was exposed to the sucrose solutions of different concentrations [14]. As the RI calibration curve is linear (Figure S3), it is reasonable to assume that the calibration curve could be used to determine the changes in RI of the film in response to exposure to ammonia. The RI calibration curve and the relationship between the RI and the wavelength of the second resonance band at a given concentration of ammonia gas could be used to calculate an equivalent RI of the TSPP film at the exposure to ammonia (see Figure S4). The RIs for the HCl-vapor-treated 15 deposition cycle film before and after the film was exposed to ammonia were estimated to be 1.4643 and 1.3585, respectively (Figure S4a). This significant change in the RI when the PDDA/TSPP film was exposed to ammonia was most likely caused by morphological changes in the TSPP in the film, from *J*- and *H*-aggregates to monomers. Hasegawa et al. [23] estimated that the RI of a TSPP monolayer formed at a toluene/water interface was 1.42. However, this value cannot be directly compared with the RI (1.4643) for the HCl-treated film because Hasegawa et al. determined the RI at a wavelength of 481 nm, which is quite different from the wavelength used in our study (approximately 800 nm).

Interestingly, the LPG sensor's response to humidity is negligible as compared its response to the ammonia-induced changes. This is a major advantage of the current LPG sensor because most commercial sensors suffer from a pronounced cross-sensitivity to humidity. The response of the sensor could be also restored by exposing the sensor to HCl vapor, which caused the monomeric TSPP that had been deprotonated by ammonia to reform *J*-aggregates. The response was completely restored when HCl vapor produced by an aqueous 0.1 M HCl solution was used, as is shown in the inset in Figure S4b. The RI of the film was completely restored, from 1.3585 to 1.4643, by this HCl treatment (Figure S4b).

3.3.4 Influence of film thickness

The LPGs were modified with PDDA/TSPP films of six, nine, and fifteen deposition cycles and were tested to determine the effect of the film thickness on the sensor performance. The changes found in the TSs of the LPGs with different film thicknesses are shown in Figure 7. The sensor with a 15-deposition-cycle film was more sensitive than the other sensors. The shift in the wavelength of the second resonance band when the most sensitive sensor was exposed to 100 ppm ammonia was estimated to be about 16 nm (Figures 7c and 7d), which was approximately four times greater than the wavelength shift found when the sensor with a film comprising nine deposition cycles was exposed to 100 ppm ammonia (less than 4 nm, Figures 7b and 7d). The transmission changes for the first resonance band followed a similar trend. The improved sensitivity to ammonia of the LPG coated with the thicker film may have been caused by the number of sites to which ammonia could become bound being higher in the thicker film. The response increased exponentially as the film thickness increased.

3.4. Ammonia gas sensing mechanism

The mechanism through which the LPG sensor modified with a PDDA/TSPP film sensed ammonia is shown in Figure 8. Initially, the TSPP molecules will be adsorbed mainly in the form of *J*-aggregates on the PDDA layer. Exposure of the TSPP to ammonia gas will lead to the TSPP being deprotonated and returning to the monomeric state. This distorts and dilutes the *J*-aggregates, decreasing the RI of the film and changing the TS of the film. The TSPP will become protonated again when the PDDA/TSPP film is exposed to HCl vapor, and the *J*-aggregates will reform within the film, increasing the RI.

As is clear from the UV–vis spectra shown in Figure 8, the TSPP can be converted between H_2TSPP^{2-} and $TSPP^{4-}$ by the protonation and deprotonation reactions caused by the presence of HCl and ammonia. Repeated exposure of the film to ammonia and HCl will cause NH_4Cl to be produced as a by-product; however, the NH_4Cl can easily be removed by washing the film with water whenever necessary. Usually, the monomeric $TSPP^{4-}$ (free base form) that is produced under pH conditions higher than 4.8 shows a strong Soret band at 413 nm, whereas below pH 4.8 the Soret band is red-shifted to 435 nm, indicating that the monomeric H_2TSPP^{2-} (diacidic form) is formed [19, 20]. The zwitterionic porphyrin H_2TSPP^{2-} in the film, to which the absorption band at around 434 nm is attributed, can form a *J*-aggregate because of electrostatic interactions between the protonated pyrrole rings and sulfonic acid groups. When this occurs, a Soret band is produced at 485 nm and a Q-band is produced at 700 nm. Ammonia molecules will be transformed into ammonium ions by receiving protons from the TSPP *J*-aggregate. This will cause the two *J*-aggregation absorption bands to completely disappear and the film only to give an absorption band for the free base monomer ($TSPP^{4-}$) at about 410 nm.

4. Conclusions

The use of a novel LPG fiber sensor modified with a film of alternating PDDA and TSPP layers to s detect ammonia gas was demonstrated. The sensor was highly selective toward ammonia gas, and the sensing mechanism depends on the TSPP in the film undergoing morphological changes, leading to changes in the wavelengths and absorbances of characteristic UV–vis absorption bands. One advantage of the proposed device is that it provides wavelength-encoded information on the binding of ammonia at wavelengths above 750 nm, along with information on changes in the transmission intensity associated with TSPP aggregate structures in the film. Another noteworthy point about this approach is that the optimal film thickness (i.e., giving the best sensitivity) can be precisely controlled because the film is produced using the layer-by-layer method. A high RI (1.4643) was achieved using a PDDA/TSPP film produced using 15 deposition cycles, and the RI decreased dramatically (to 1.3585) when this film was exposed to ammonia. This sensor system could be used as a new biosniffer for the sensitive and selective detection of amine odors in the environment or produced by the human body, since the sensor response is shows a very low sensitivity to humidity.

Acknowledgments

This work was supported by MEXT via the 2nd Kitakyushu Knowledge-based Cluster Project. The authors would also like to acknowledge the support of a UK Engineering and Physical Sciences Research Council Platform Grant (EP/H02252X/1) and a responsive mode grant (EP/L010437/1).

References

1. American Industrial Hygiene Association: Ammonia, Hygienic Guide Series, Detroit, Michigan (1971).
2. http://www.cdc.gov/niosh/topics/ammonia/, accessed 27/01/2015.
3. I.D. Weiner, W.E. Mitch, J.M. Sands, Urea and Ammonia Metabolism and the Control of Renal Nitrogen Excretion, Clinical Journal of the American Society of Nephrology, (2014) CJN 10311013.
4. F.M. Schmidt, O. Vaittinen, M. Metsälä, M. Lehto, C. Forsblom, P.H. Groop, and L. Halonen, Ammonia in breath and emitted from skin, Journal of Breath Research, 7 (2013) 017109.
5. L.R. Narasimhan, W. Goodman, C.K.N. Patel, Correlation of breath ammonia with blood urea nitrogen and creatinine during hemodialysis, Proceedings of the National Academy of Sciences of the United States of America, 98 (2001) 4617–4621.
6. J.P. Ong, A. Aggarwal, D. Krieger, K.A. Easley, M.T. Karafa, F. Van Lente, et al., Correlation between ammonia levels and the severity of hepatic encephalopathy, American Journal of Medicine, 114 (2003) 188–193.
7. J.G. Kusters, A.H.M. Van Vliet, E.J. Kuipers, Pathogenesis of Helicobacter pylori infection, Clinical Microbiology Reviews, 19 (2006) 449–490.
8. A. Tangerman, E.G. Winkel, Extra-oral halitosis: An overview, Journal of Breath Research, 4 (2010) 017003.
9. C. Turner, P. Španěl, D. Smith, A longitudinal study of ammonia, acetone and propanol in the exhaled breath of 30 subjects using selected ion flow tube mass spectrometry, SIFT-MS, Physiological Measurement, 27 (2006) 321–337.
10. B. Timmer, W.A. Olthuis, Ammonia sensors and their applications—a review,

Sensors and Actuators B: Chemical, 107 (2005) 666–677.

11. T. Wang, S. Korposh, R. Wong, S. James, R. Tatam, S.-W. Lee, A novel ammonia gas sensing using a nano-assembled polyelectrolyte thin film on fiber optic long period gratings, Chemistry Letters, 41 (2012) 1297–1299.
12. T. Wang, S. Korposh, S. James, R. Tatam, S.-W. Lee, Optical fiber long period grating sensor with a polyelectrolyte alternate thin film for gas sensing of amine odors, Sensors and Actuators B: Chemical, 185 (2013) 117–124.
13. S. Korposh, T. Wang, S. James, R. Tatam, S.-W. Lee, Pronounced aromatic carboxylic acid detection using a layer-by-layer mesoporous coating on optical fibre long period grating, Sensors and Actuators B: Chemical, 173 (2012) 300–309.
14. S. Korposh, S.-W. Lee, S.W. James, R.P. Tatam, Refractive index sensitivity of fibre optic long period gratings coated with SiO_2 nanoparticle mesoporous thin films, Measurement Science and Technology, 22 (2011) 075208.
15. S. Korposh, S.W. James, S.-W. Lee, S. Topliss, S.C. Cheung, W.J. Batty, R.P. Tatam, Fiber optic long period grating sensors with a nano-assembled mesoporous film of SiO_2 nanoparticles, Optics Express, 18 (2010) 13227–13238.
16. S.W. James, R.P. Tatam, Optical fibre long-period grating sensors: Characteristics and application, Measurement Science and Technology, 14 (2003) R49–R61.
17. S.C. Cheung, S.M. Topliss, S.W. James, R.P. Tatam, Response of fibre optic long period gratings operating near the phase matching turning point to the deposition of nanostructured coatings, Journal of the Optical Society of America B, 25 (2008) 897–902.
18. S. Korposh, S. Kodaira W. Batty, S.W. James, S.-W. Lee, Nanoassembled thin-film gas sensor II. An intrinsic highly sensitive fibre optic sensor for ammonia

detection, Sensors and Materials, 21 (2009) 179–189.

19. D.L. Akins, H.-R. Zhu, C. Guo, Absorption and Raman scattering by aggregated meso-tetrakis(p-sulfonatophenyl)porphine, Journal of Physical Chemistry, 98 (1994) 3612−3618.
20. O. Ohno, K. Kaizu, H. Kobayashi, J-Aggregate formation of a water-soluble porphyrin in acidic aqueous media, Journal of Chemical Physics, 99 (1993) 4128−4139.
21. A.S.R. Koti, J. Taneja, N. Periasamy, Control of coherence length and aggregate size in the J aggregate of porphyrin, Chemical Physics Letters, 375 (2003) 171−176.
22. J.L. McHale, Hierarchal light-harvesting aggregates and their potential for solar energy applications, Journal of Physical Chemistry Letters, 3 (2012) 587−597.
23. Y. Moriya, T. Hasegawa, T. Okada, N. Ogawa, E. Kawai, K. Abe, M. Ogasawara, S. Kato, S. Nakata, Analysis of Gibbs monolayer adsorbed at the toluene/water interface by UV-visible partial internal reflection spectrometry, Analytical Chemistry, 78 (2006) 7850–7856.

Figure Captions

Figure 1. Schematic of the deposition of a film containing PDDA and TSPP onto an LPG optical fiber.

Figure 2. Changes in the transmission spectra of the LPG optical fiber as the number of layers deposited (marked next to each line) increased, when the outermost layer was (a) PDDA and (b) TSPP.

Figure 3. Dependence of the wavelength shifts (a and b) and the transmission changes (c and d) for the first and second resonance bands on the number of deposition cycles performed.

Figure 4. UV–vis absorption spectra of a PDDA/TSPP alternate film produced using five deposition cycles when the outermost layer was (a) PDDA and (b) TSPP. The insert in (b) shows the relationships between the absorbances at 429, 485, and 700 nm and the number of deposition cycles performed.

Figure 5. UV–vis absorption spectra of a PDDA/TSPP film deposited using five cycles before and after the film was exposed to HCl vapor produced by a 0.1 M HCl solution, and transmission spectra of a PDDA/TSPP film deposited using 15 cycles before and after the film was exposed to HCl vapor produced by a 0.1 M HCl solution.

Figure 6. (a) Changes in the transmission spectra and (b) responses of the sensor when the LGP sensor coated with a PDDA/TSPP film produced using 15 deposition cycles was exposed to ammonia gas, where 0 ppm means pure water vapor (containing no ammonia).

Figure 7. Transmission spectra of LPG sensors modified with PDDA/TSPP films produced using (a) six, (b) nine, and (c) fifteen deposition cycles before (blue lines) and after (red lines) the sensors were exposed to 100 ppm ammonia. (d) Comparison of the wavelength shifts and the transmission changes obtained using the sensors with films produced using six, nine, and fifteen deposition cycles.

Figure 8. (a) Evolution of the UV–vis absorption spectrum of a PDDA/TSPP film produced using five deposition cycles on a quartz plate. The black line is for the

as-prepared film, the green line for the film after it had been exposed to HCl vapor produced by a 1.0 M HCl solution, and the blue line is for the film after it had been exposed to ca. 500 ppm ammonia gas. (b) Schematic of the mechanism through which the PDDA/TSPP film deposited on an LPG fiber senses ammonia.

Figure 1

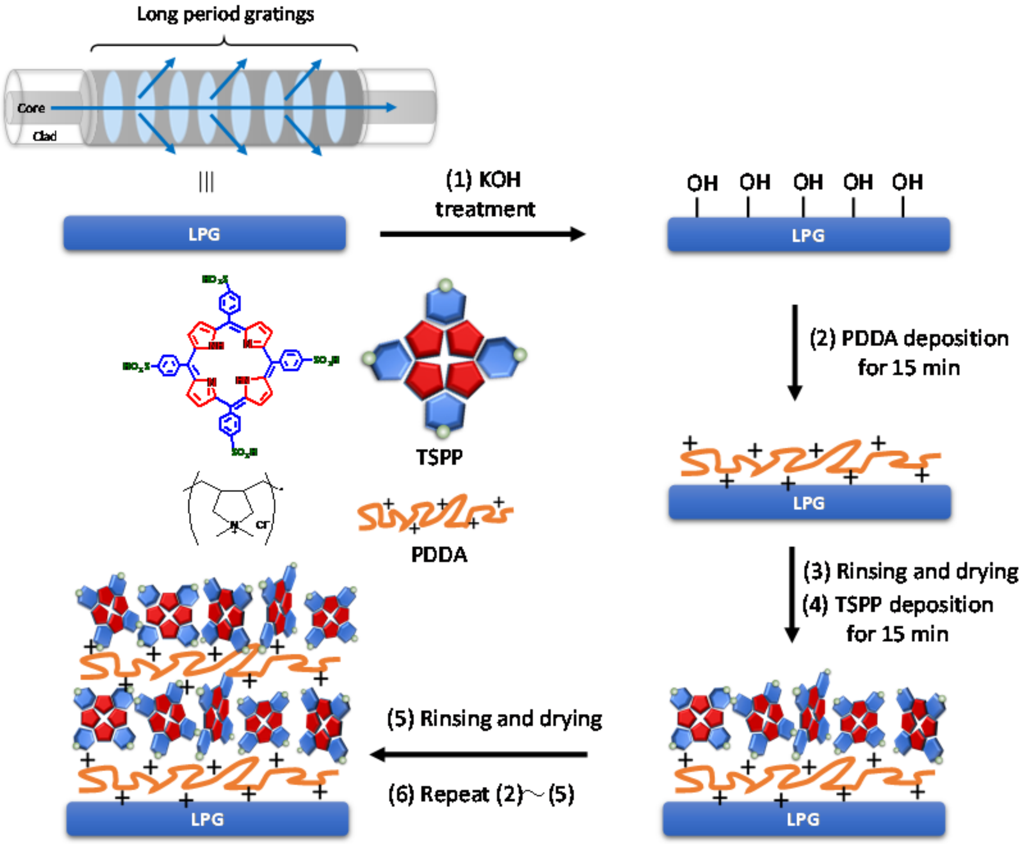
Long period gratings
Core
Clad
LPG
(1) KOH treatment
OH OH OH OH OH
LPG
(2) PDDA deposition for 15 min
LPG
TSPP
PDDA
(3) Rinsing and drying
(4) TSPP deposition for 15 min
LPG
(5) Rinsing and drying
(6) Repeat (2)~(5)
LPG

Figure 2

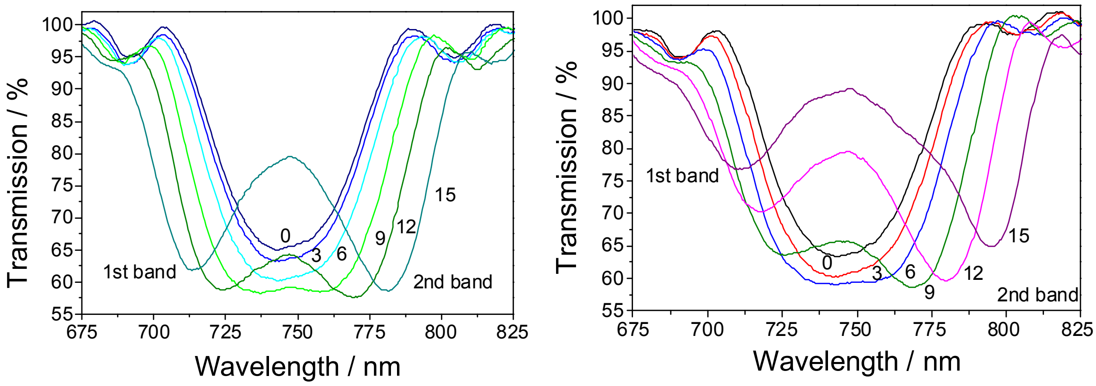
Transmission / %
100
95
90
85
80
75
70
65
60
55
675
700
725
750
775
800
825
Wavelength / nm
1st band
2nd band
0
3
6
9
12
15

(a) (b)

Figure 3

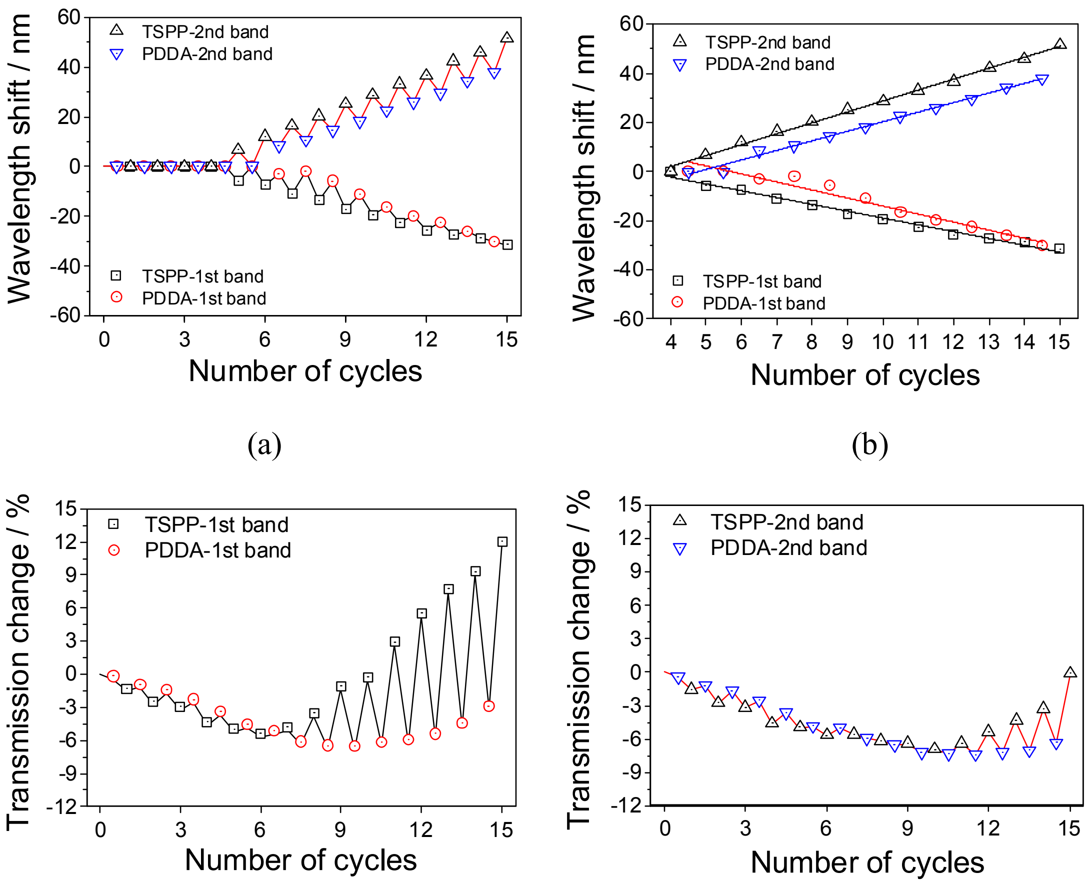

(a)

(b)

(c)

(d)

Figure 4

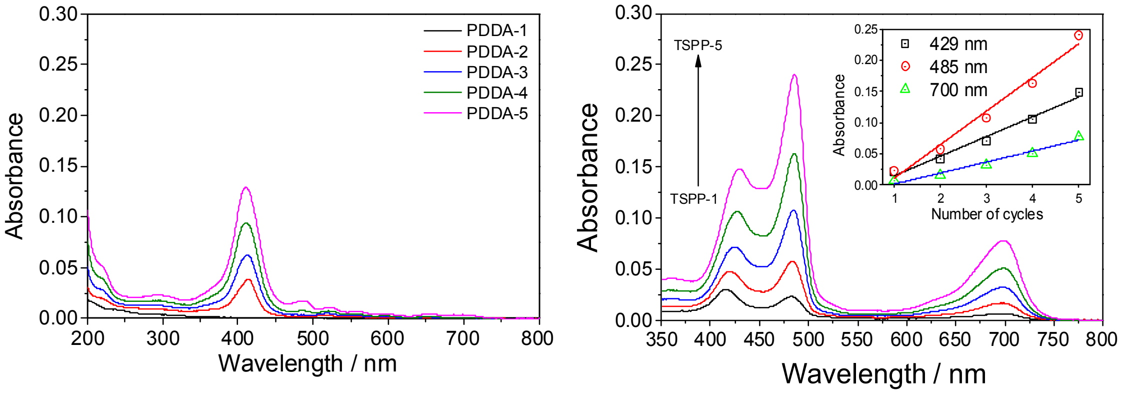
Absorbance
0.30
0.25
0.20
0.15
0.10
0.05
0.00
200
300
400
500
600
700
800
Wavelength / nm
PDDA-1
PDDA-2
PDDA-3
PDDA-4
PDDA-5
TSPP-5
TSPP-1
350
400
450
500
550
600
650
700
750
800
429 nm
485 nm
700 nm
Number of cycles
1
2
3
4
5

(a) (b)

Figure 5

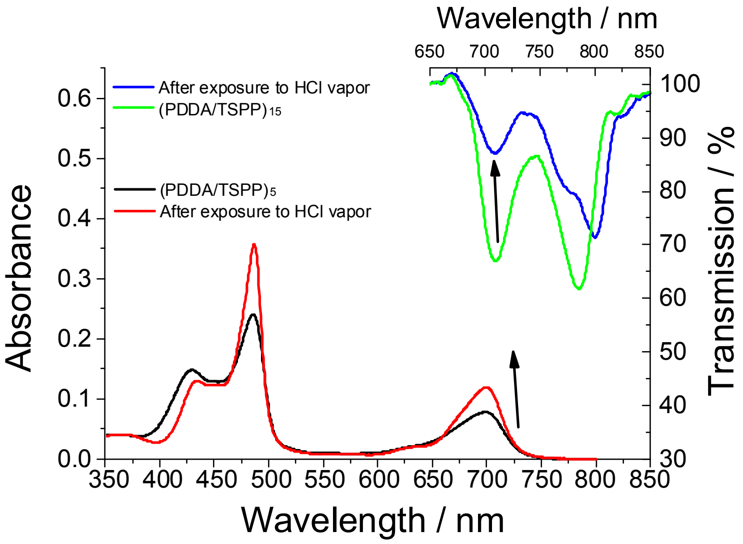
Wavelength / nm
650
700
750
800
850
After exposure to HCl vapor
(PDDA/TSPP)15
(PDDA/TSPP)5
After exposure to HCl vapor
Absorbance
0.0
0.1
0.2
0.3
0.4
0.5
0.6
Transmission / %
30
40
50
60
70
80
90
100
350
400
450
500
550
600
650
700
750
800
850
Wavelength / nm

Figure 6

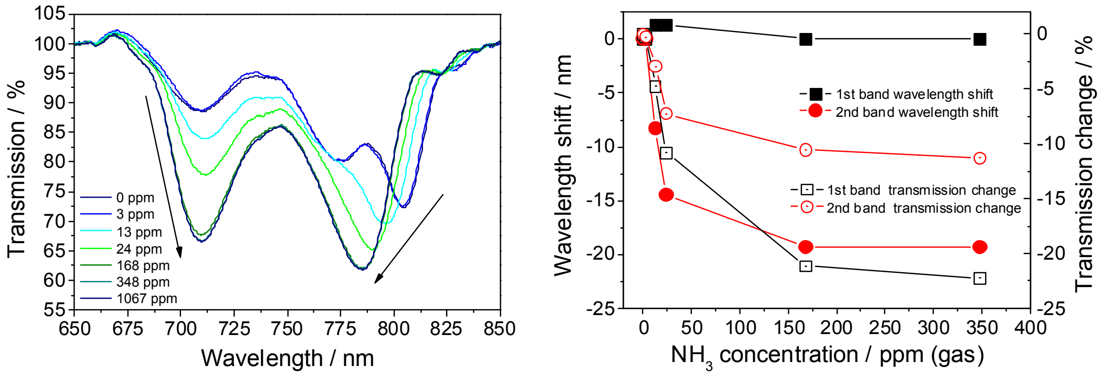
Transmission / %
105
100
95
90
85
80
75
70
65
60
55
650
675
700
725
750
775
800
825
850
Wavelength / nm
0 ppm
3 ppm
13 ppm
24 ppm
168 ppm
348 ppm
1067 ppm
Wavelength shift / nm
0
-5
-10
-15
-20
-25
0
50
100
150
200
250
300
350
400
NH$_3$ concentration / ppm (gas)
Transmission change / %
0
-5
-10
-15
-20
-25
1st band wavelength shift
2nd band wavelength shift
1st band transmission change
2nd band transmission change

(a) (b)

Figure 7

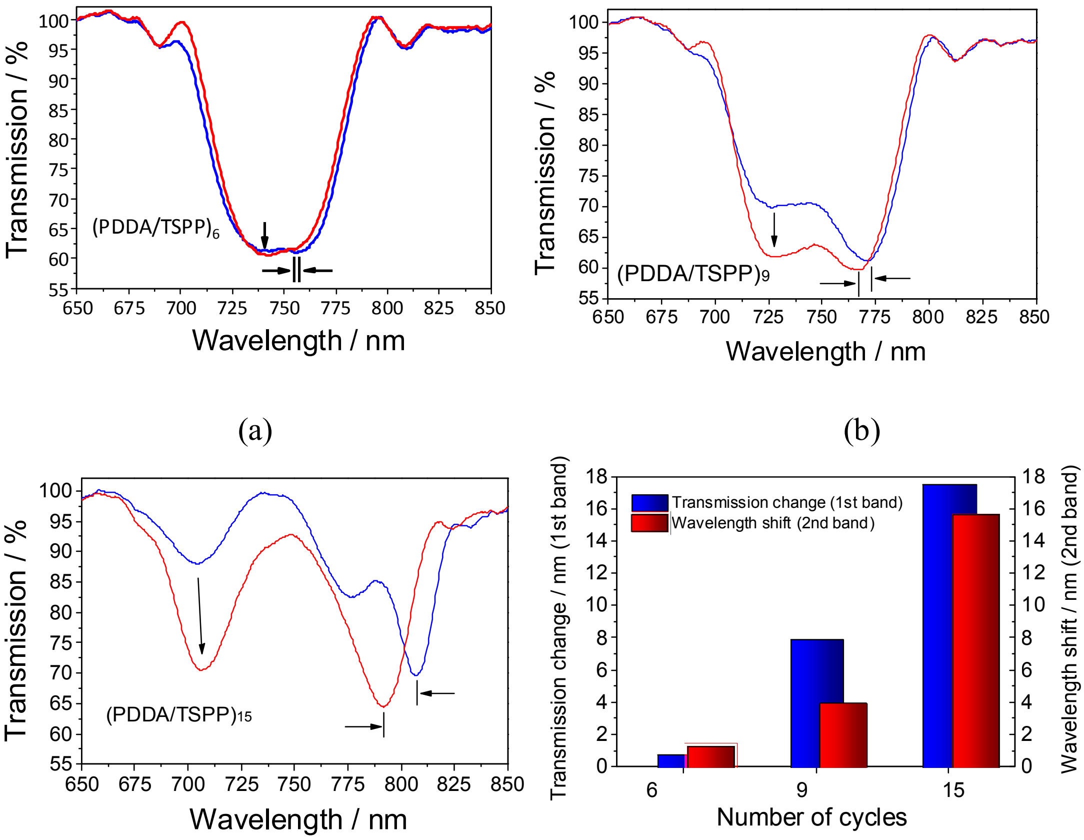

(a) (b)

(c) (d)

Figure 8

(a)

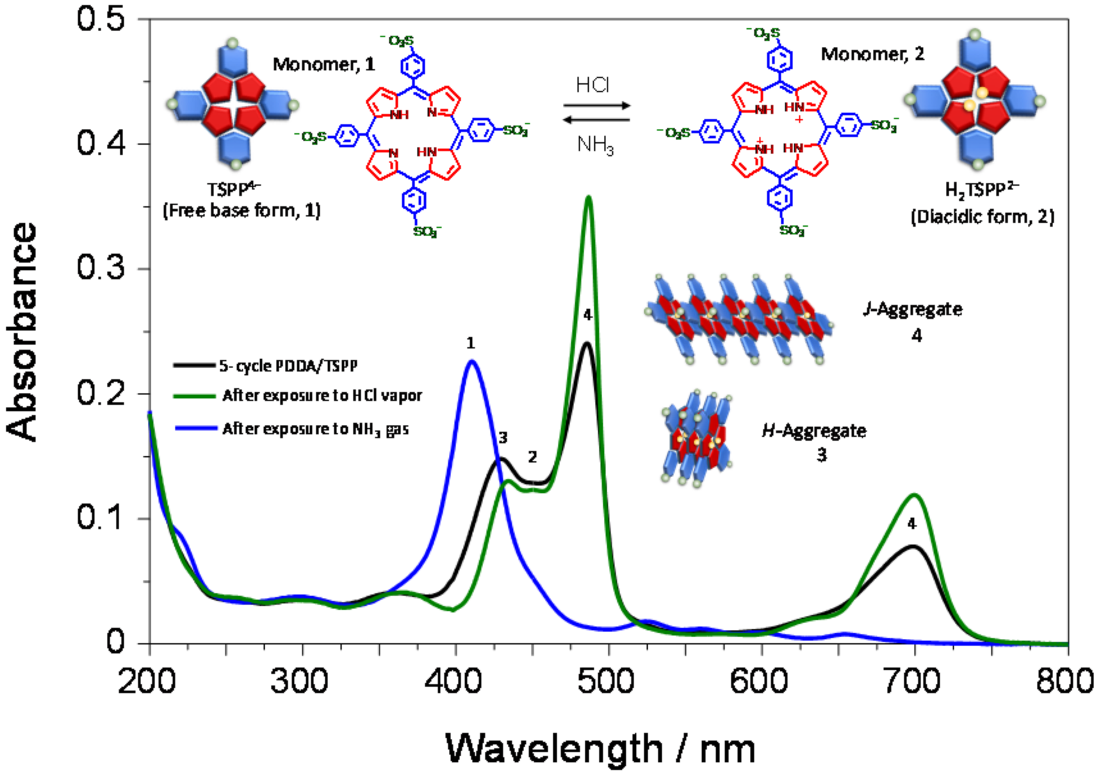
Absorbance
Wavelength / nm
0
0.1
0.2
0.3
0.4
0.5
200
300
400
500
600
700
800
Monomer, 1
TSPP4−
(Free base form, 1)
HCl
NH3
Monomer, 2
H2TSPP2−
(Diacidic form, 2)
J-Aggregate
4
H-Aggregate
3
5-cycle PDDA/TSPP
After exposure to HCl vapor
After exposure to NH3 gas
1
2
3
4
4

(b)

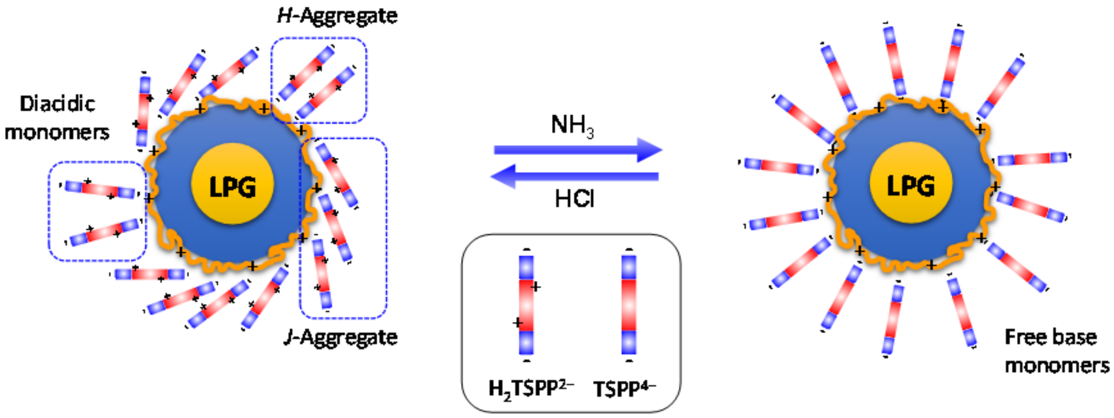
H-Aggregate
Diacidic monomers
LPG
J-Aggregate
NH3
HCl
H2TSPP2−
TSPP4−
LPG
Free base monomers